Proceedings of ASME 2023
5th International Offshore Wind Technical Conference
IOWTC2023
December 18-19, 2023, The Exeter University, Exeter, United Kingdom

IOWTC2023-119381

AERO-HYDRODYNAMIC STUDIES OF A 15 MW SEMI-SUBMERSIBLE FOWT TO ASSESS THE SUITABILITY OF THE INCLUSION OF A DAMPER SYSTEM

Yu Gao
Renewable Energy Group, Faculty of Environment, Science, and Economy, University of Exeter, Penryn, Cornwall, UK

Chenyu Zhao
Renewable Energy Group, Faculty of Environment, Science, and Economy, University of Exeter, Penryn, Cornwall, UK

Lars Johanning
Renewable Energy Group, Faculty of Environment, Science, and Economy, University of Exeter, Penryn, Cornwall, UK

Ajit C Pillai
Renewable Energy Group, Faculty of Environment, Science, and Economy, University of Exeter, Penryn, Cornwall, UK

ABSTRACT

Floating offshore wind turbines can exploit the high energy density experienced in offshore environments, with turbines now reaching up to 15 MW in size. However, given the larger size of these turbines and the severe offshore environment, there remains significant challenges in motion stabilization. To overcome these challenges, the inclusion of a damper system could be considered to reduce motions. This paper conducts a numerical dynamic analysis of a 15 MW semi-submersible floating offshore wind turbine under a range of environmental conditions, informing the design criteria for such a damper system. The study presents the findings under different environmental loading conditions. In the first instance, the time-domain results of hydrodynamic study were used to determine the dominant characteristics. The initial study identified the pitch motion of main concern. The simulations were carried out under wave-only and wind-wave loading. In the wave-only conditions study, excitation modes were observed at both the eigenfrequency and excitation frequency, dependent on wave conditions. When the wind loads were introduced, a large mean pitch offset and amplitude relative to the mean offset were observed. Within the discussion, a dual damper system is suggested to increase the stability of the platform.

Keywords: Floating offshore wind turbine, hydrodynamic, aerodynamic, damper system, Orcaflex

1. INTRODUCTION

Offshore wind power, as a clean energy resource, has presented a significant contribution to the development of energy from renewable energy sources. This attractive and competitive source has overwhelming advantages over alternate renewable energy technologies, including solar, tidal, and wave energy [1]. Compared to onshore wind energy, offshore wind energy, is almost three times more efficient than onshore wind energy, and are more effective due to the more consistent winds in offshore environments [2], [3]. With the continuous advancement of technology, the Offshore Wind Turbines (OWTs) have evolved to become larger in size and are now deployed in deeper sea depth. At depths beyond 50 m, bottom-fixed supporting structures cease to be economically viable [4]. As a result, floating offshore wind turbines (FOWTs) have emerged as a viable option to harness wind power in deeper offshore areas [5].

In general, the FOWT presents a significant challenge towards motion stabilization due to the complex environmental loads, including wave, wind, and current loads and the increasing size. These forces can cause undesirable high and low order motions [6]. The wave loads, including second-order wave loads, could excite the platform pitch resonance, which could cause structural failures [7]. Due to the turbulent aerodynamic and hydrodynamic loads, the wind turbine tower vibration can be significant and has a noticeable impact on downtime, the lifetime of the components, and even the overall integrity of the FOWT [8]. Additionally, the wind loads can be prominent in the surge, pitch motions, and tower bending moments with the increasing size of the wind turbine [9]. Therefore, it is highly important to study the motion responses of FOWTs and search for engineering solutions to eliminate undesirable motions and improve system reliability.

Multiple studies have been conducted exploring damper devices for FOWT applications [10]. Basu et al. [11] verified the effectiveness of a tuned liquid column damper (TLCD) mitigating the vibrations for monopile fixed OWT. Lackner et al. [12], [13] investigated passive structural control of various types for 5 MW FOWTs, including barge, spar, and tension leg

platforms, using a simplified model. The results showed that the tuned mass damper (TMD) is efficient in the vibration reduction of FOWTs, especially in side-to-side tower bending. Li et al. [14] implemented TMDs to reduce the vibrations of the platform and tower. The lower stiffness TMDs can dissipate the energy of platform pitch vibration, and the higher stiffness TMDs absorb the energy of tower bending. Furthermore, Hemmati et al.[15] studied the effectiveness of a combined TLCD and TMD system on the vibration reduction of OWTs. The results demonstrated that the TMDs are more efficient in operating conditions.

Active dampers are effective in reducing structural loads and vibrations, but at the expense of active power and large stroke [16]. Brodersen et al. [17] employed an active tuned mass damper (ATMD) for fixed OWTs to investigate its effect on tower vibrations. The authors concluded that the ATMD is highly efficient in reducing the tower vibrations in transient conditions. Hu and He [18] investigated the active control for barge-type FOWT. In this study, the ATMD was limited by a stroke-limited hybrid mass damper. Fitzgerald et al. [19] studied the effect of an ATMD on onshore wind turbines. The results demonstrated that the ATMD presents a significant improvement in the reliability of the wind turbine at the rated speed.

This paper provides a dynamic analysis of wave and wind loading on the IEA 15 MW FOWT installed on a semi-submersible structure, focusing on the response characteristics of the moored system in order to inform the design of a suitable active or passive damper that would enhance the stability. The numerical analysis is conducted under various wave and wind conditions using Orcaflex [20] while taking into account the wave drift loads. Key response frequencies for different wave periods and heights are assessed to inform about suitable damper solutions. The dynamic response characteristics for different wind-wave conditions are identified. Furthermore, the effect of aerodynamics is discussed.

This paper is organized as follows: Section 2 describes the numerical model, and key parameters; Section 3 presents the analysis results of the hydrodynamic study in time-domain, frequency-domain, and aero-hydrodynamic study; Section 4 suggests a potential damper system and future work; and Section 5 presents the conclusion.

2. NUMERICAL STUDY

2.1 Governing equations

This study employs the IEA 15 MW semi-submersible FOWT, shown in FIGURE, designed by National Renewable Energy Laboratory, Technical University of Denmark, and University of Maine. Equation 1 is the overarching motion equation of the structure.

$$M\ddot{X}(t) + \int_{-\infty}^{t} L(t-\tau)\dot{X}(\tau)d\tau + KX(t) = F_e \qquad (1)$$

Where M is the mass matrix, consisting of the structural mass, and added mass matrix; $L(t-\tau)$ is the retardation function matrix, including frequency dependent added mass and damping terms. B is the damping matrix including viscous damping B_v causing viscous drag loads, radiation damping B_r, and structural damping B_s; K is the component of stiffness matrix which are mooring stiffness K_m, and hydrostatic stiffness K_h (hydrostatic restoring force); $\ddot{X}(t)$, $\dot{X}(t)$, $X(t)$ are acceleration, velocity, and displacement of structure respectively; F_e is the external loads, including hydrodynamic and aerodynamic forces.

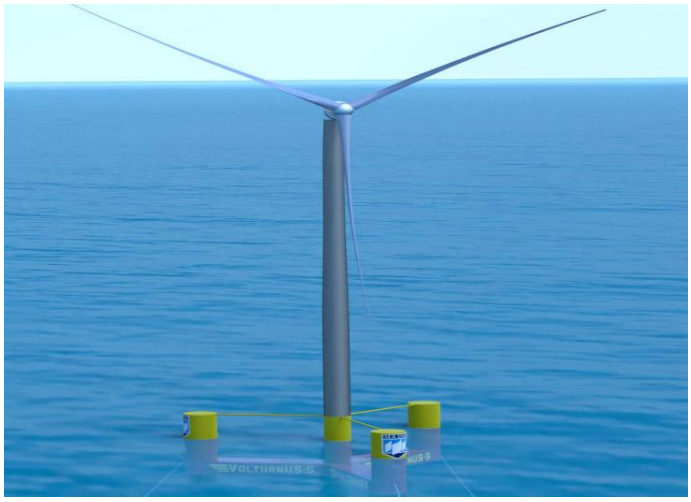

FIGURE 1: THE UMAINE VOLTURNUS-S REFERENCE PLATFORM TO SUPPORT 15 MW TURBINE [21].

In this study, the Morison equation and diffraction theory are both considered to take into account the viscous drag force [22] calculating the first-order wave loads including drag loads, incident wave loads, diffraction loads, and radiation loads. Additionally, the second-order wave loads are considered as semi-submersibles are sensitive to the second-order wave effects especially wave drift loads [7]. The second-order wave loads, proportional to the square of wave amplitude, can be divided into two parts: difference-frequency loads (wave drift loads) and sum-frequency loads. The sum-frequency loads are excluded as they have negligible effects on the substructure according to [23]. The wind loads in this study are calculated by using Blade Element Momentum (BEM) theory to account for the axial and tangential induction factors.

2.1 THE KEY PARAMETERS OF THE FOWT

The IEA 15 MW FOWT utilizes the UMaine VolturnUS-S reference platform [24], which was designed by the University of Maine specifically to support the IEA 15 MW reference wind turbine.

The key parameters of the FOWT can be seen in [24]. The platform is a steel semi-submersible with a draft of 20 m, designed for deployment in 200 m of water depth. The wind turbine system [21] consists of two separate components, the tower and the rotor and nacelle assembly (RNA). The height of the tower reaches 150 m, which allows 30 m of water surface clearance. The blade length of the reference turbine is 117 m with a root diameter of 5.2 m, and the mass of the blade is 65 tons.

The mooring system properties are presented in Table 1[24]. For the mooring system, the finite element solution is adopted to calculate the loads applied by the mooring system, as it can obtain a realistic approximation with high accuracy.

TABLE 1: MOORING SYSTEM PROPERTIES[24].

Parameter	Value	Unit
Type	Chain Catenary	-
Number	3	-
Anchor Depth	200	m
Fairlead Depth	14	m
Anchor Radial Spacing	837.6	m
Fairlead Radial Spacing	58	m
Nominal Chain Diameter	185	mm
Dry Line Linear Density	685	kg/m
Extensional stiffness	3,270	MN
Fairlead Pretention	2,437	kN

2.2 NUMERICAL MODEL SETUP

In Orcaflex, the floating foundation is modelled connected with three pontoons as having 6-DOF considering the effects of first-order wave loads, wave drift loads, wave drift damping and added mass. The mass of pontoons is zero as they are assumed to be built into the substructure. The other damping, accounting for the quadratic damping coefficients applied to the platform motions, is added in the analysis. The properties of the platform are obtained by a diffraction analysis in OrcaWave considering the full system including tower, nacelle, and rotor.

The blades and tower are modelled by the line elements with considering the structural damping and stiffness. The nacelle and hub are modelled in OrcaFlex as 6-DOF buoys with mass and inertia. The tower is divided into 26 segments each measuring 5 m in length. The connection between the tower and the substructure is assumed to be rigid. The mooring lines are discretized into 85 sections each of 10 m length. The azimuth between the lines are 120 degrees. The finite element method is used to calculate the mooring loads.

Newman's approximation method [7] is chosen to calculate the second-order wave forces. This approximation only considers the diagonal values of the full quadratic transfer function (QTF) and avoids computing the second-order velocity, which can improve the computational efficiency and, at the same time, maintain the accuracy. The Gonalez model is used to account for unsteady aerodynamic model.

In this study, the direction of the incident wave is 180 degrees heading to the wind turbine seen in Fig. 2, defined by the JONSWAP spectrum with a crest factor of 3.3. The full field wind is generated by using Turbsim [25] to obtain the turbulence model. Particularly, the wind speed is set to zero when investigating the wave effects. The simulations are executed for 3600 s with a 400-seconds build-up stage to eliminate any start-up transient effects. The dynamic time step is 0.025 s.

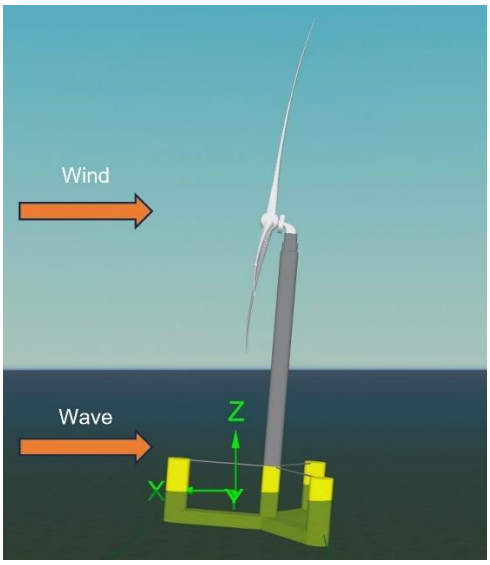

FIRGURE 2: THE DIAGRAM OF THE WIND AND WAVE DIRECTION.

2.3 NATURAL FREQUENCIES OF THE FOWT

The natural frequencies, seen in Table 2, were obtained from the module of the modal analysis in Orcaflex [26], [27]. The modal analysis calculates the undamped natural modes of a system, characterized by their modal frequency and mode shape. The undamped natural modes represent that the added mass and radiation damping are neglected in this process, as it is difficult to account for the frequency dependent data.

In this study, the average added mass and radiation damping matrixes of the platform under the infinite frequency, only considering the diagonal elements, are supplied for a more accurate natural frequency calculation.

TABLE 2: NATURAL FREQUENCIES OF THE FOWT.

Parameter	Frequency	Period
Surge	0.008 Hz	125 s
Sway	0.007 Hz	143 s
Heave	0.046 Hz	22 s
Roll	0.035 Hz	28 s
Pitch	0.036 Hz	27.78 s
Yaw	0.012 Hz	83 s

2.4 ENVIRONMENTAL LOADING CASES

The designed load cases are selected based on the 25-year measurements of Gran Canaria. The higher significant wave heights (H_s) of 5.4 m, 6 m, and 7.1 m are introduced to serve as extreme wave conditions. Therefore, the range of significant wave height is 2.5 m to 7.1 m. According to Table 2, the natural period of the structural pitch is approximately 28 s. Additionally, to investigate the effect of varying peak period on the wind turbine motion, an extended range of spectral peak periods (T_p) from 4.98 s to 28 s is selected

3. RESULTS AND DISCUSSION

This section presents the results of the dynamic analysis in time and frequency domains, including wave-only and wave-wind conditions.

3.1 IDENTIFICATION OF CRITICAL MOTIONS

The details of the cases for hydrodynamic study can be found in Table 3 and Table 4. The time-domain results of cases 1-30 determine the key motions of the FOWT in 6 DOFs. Cases 1-6 are used to investigate motion responses of the FOWT by sharing the same wave period and different significant wave heights. Similarly, cases 7-13 and 19-25 explore the wave period effects by using the same significant wave height and different wave periods.

TABLE 3: DESIGN LOAD CASES WITH A RANGE OF WAVE HEIGHTS AT PEAK PERIOD 8 S.

Case number	Significant wave height (m)	Peak Periods (s)
1	2.5	8
2	3.6	8
3	4.2	8
4	5.4	8
5	6	8
6	7.1	8

TABLE 4: DESIGN LOAD CASES WITH A RANGE OF WAVE PERIODS AT SIGNIFICNAT WAVE HEIGHTS 4.73Mm and 7.1 M.

Case	H_s (m)	Case	H_s (m)	Peak Periods (s)
7	4.73	19	7.1	4.98
8	4.73	20	7.1	7.04
9	4.73	21	7.1	9.43
10	4.73	22	7.1	11.9
11	4.73	23	7.1	14.29
12	4.73	24	7.1	16.13
13	4.73	25	7.1	18.87
14	4.73	26	7.1	20
15	4.73	27	7.1	23.1
16	4.73	28	7.1	24.6
17	4.73	29	7.1	26.2
18	4.73	30	7.1	28

For the design of a damper system, it is critical to identify the key motions of the FOWT. Fig. 3 presents the 6 DOFs motion amplitudes of the FOWT with a range of significant wave heights at a fixed wave period of 8 s. Fig. 4 presents the 6 DOFs motion amplitudes of the FOWT with a range of wave periods at fixed significant wave heights.

The results show that the motion amplitudes of roll, yaw, and sway are close to zero with varying significant wave heights and wave periods. The surge, heave, and pitch motions are relatively more remarkable than these motions. The amplitudes of surge motion become larger with the increase in significant wave heights at fixed wave periods but smaller with the increasing of wave periods at fixed significant wave heights. The amplitudes of heave motion are not sensitive to the varying significant wave heights and wave periods compared to surge and pitch.

For the pitch motion, the results in FIGURE 3: EXTREME MOTION AMPLITUDES OF 6 DOFS UNDER CASES 1-6 (b) show that the pitch motion under different significant wave heights exhibits the same trend but with different amplitudes. In FIGURE 4: EXTREME MOTION AMPLITUDES OF 6 DOFS UNDER CASES 7-30 UNDER 1 HOUR DURATION., The pitch motion increases remarkably with the increase in wave periods. According to [28], [29], the surge and heave motions can be restricted effectively by the mooring system. If the maximum offset in the surge of the platform is less than 50% of water depth then it is acceptable [30]. Generally, heave plates can be effective and common in reducing the heave motion responses of the FOWT [31].

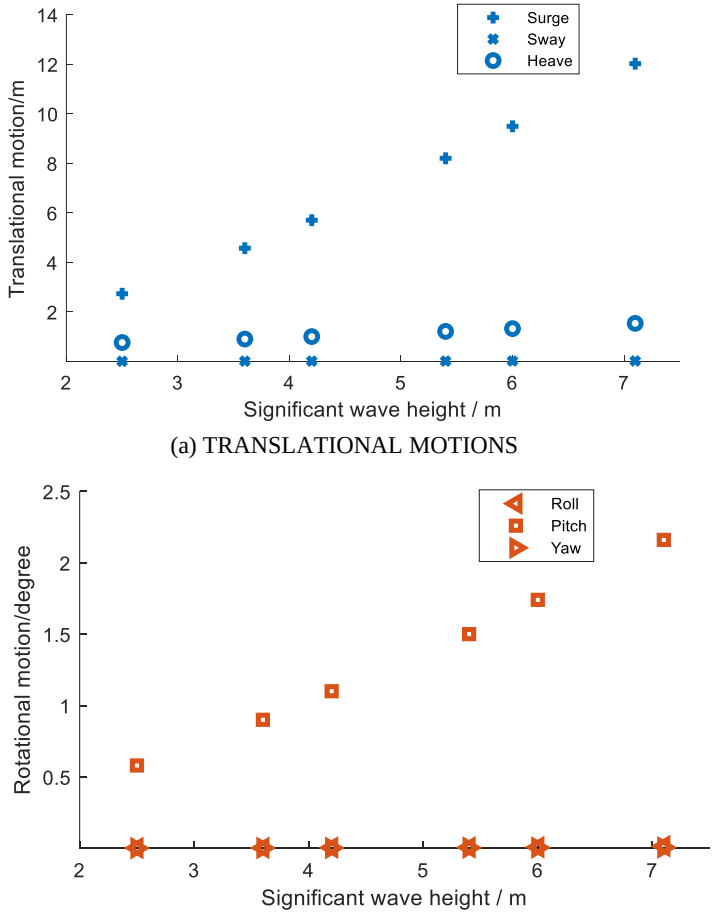

(a) TRANSLATIONAL MOTIONS

(b) ROTATIONAL MOTIONS

FIGURE 3: EXTREME MOTION AMPLITUDES OF 6 DOFS UNDER CASES 1-6 UNDER 1 HOUR DURATION.

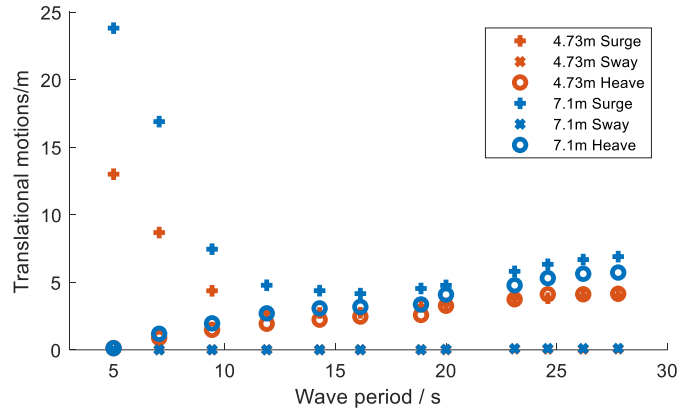

(a) TRANSLATIONAL MOTIONS

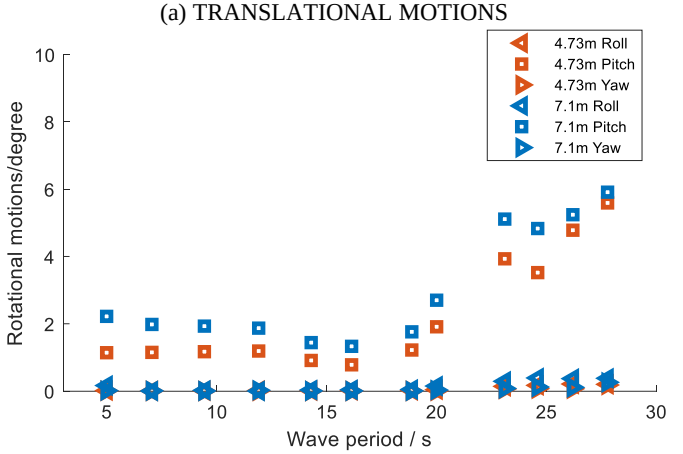

(b) ROTATIONAL MOTIONS

FIGURE 4: EXTREME MOTION AMPLITUDES OF 6 DOFS UNDER CASES 7-30 UNDER 1 HOUR DURATION.

Accordingly, the pitch motion is analyzed as the key parameter to be damped. The pitch motion results are then analyzed in the frequency domain.

3.1 HYDRODYNAMIC STUDY

Fig. 5 presents the significant wave height effects on the pitch motion of cases 1-6 at fixed wave period of 8 s. The results indicate that there are two dominant peaks in the power spectral density plots. The two peaks become more prominent when significant wave height increases. Additionally, the two peaks are almost equal in energy, particularly when the significant wave height is 7.1 m. The first peak occurs at the natural frequency of the structural pitch motion, whilst the second peak is around the wave frequency, which means it is induced by the first-order wave loads. The increasing significant wave heights have no influence on the frequencies of the two peaks.

Furthermore, it is observed that there is no first peak at the low frequency region without considering the second-order wave loads in Fig. 6. This indicates that the first peak is induced by the second-order wave loads (wave drift loads). Only one case is shown, as other cases are similar.

Fig. 7 shows the results of the two peaks with the change in the wave period under fixed significant wave heights. As illustrated in **Error! Reference source not found.**, the spectral density peak frequencies remain unchanged. Therefore, only the results of a significant wave height of 4.73 m are presented (cases 7-18). In **Error! Reference source not found.** (a), the results show that the second peak frequencies gradually approach the natural frequency with the increase in the wave period. The frequencies between the two peaks are equal when the wave period is 18.87 s. According to **Error! Reference source not found.** (b), the first peak is much larger when the wave periods are 4.98 s and 18.87 s, especially at wave period 18.87 s.

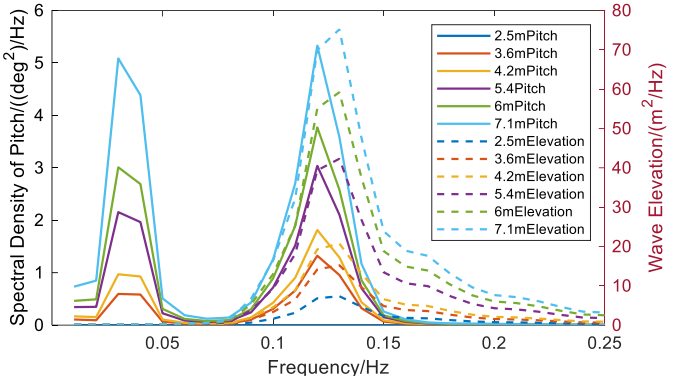

FIGURE 5: SPERTRAL DENSITY VARIATION IN PITCH MOTION AND WAVE ELEVATION UNDER CASES 1-6.

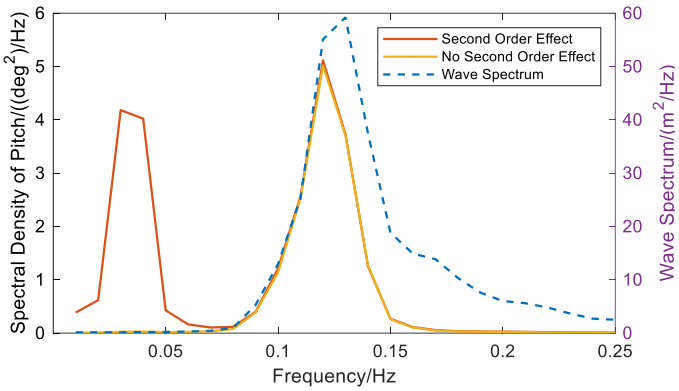

FIGURE 6: COMPARISON OF THE SPECTRAL DENSITY OF PITCH MOTION WITH AND WITHOUT THE SECOND-ORDER EFFECT UNDER CASE 19.

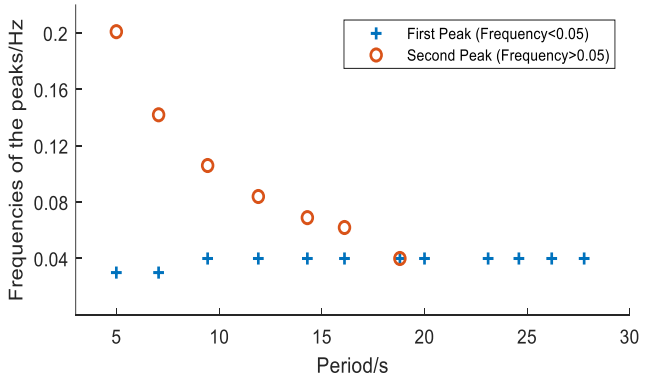

(a) Spectral density peak frequencies

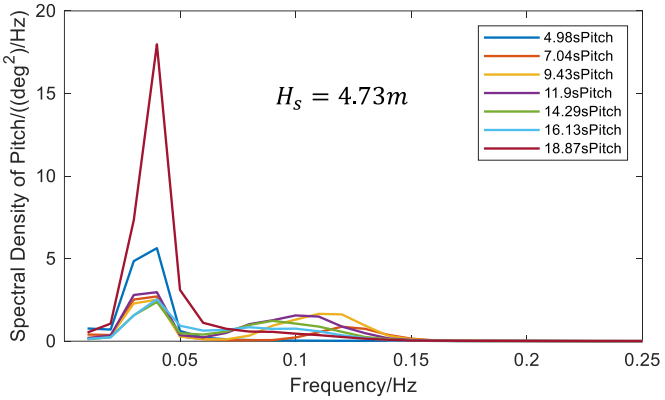

(b) Spectral density amplitude

FIGURE 7: SPECTRAL DENSITY OF PITCH MOTION WITH A RANGE OF WAVE PERIODS.

To highlight the relevant frequencies and the impact of the varying wave period, the two peaks are separated by replotting the graphs. More periods (13.1 s, 15.15 s and 17.54 s) are introduced between 4.98 s and 18.87 s to get greater granularity. The results of 7.1 m wave height are used to compare the results. Fig. 8 shows the first and second peaks in relation to the change in the wave period under fixed significant wave heights.

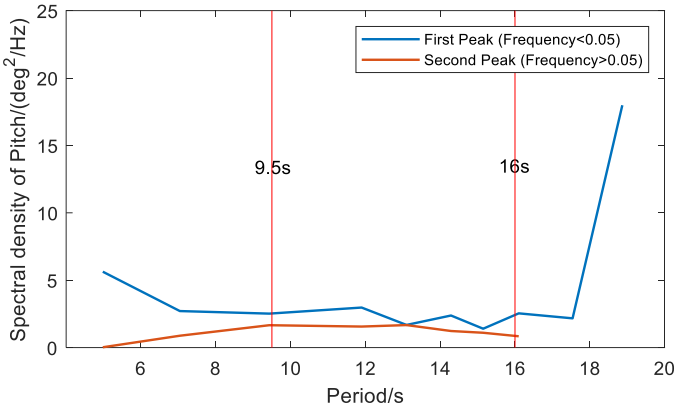

(a) $H_s = 4.73\ m$

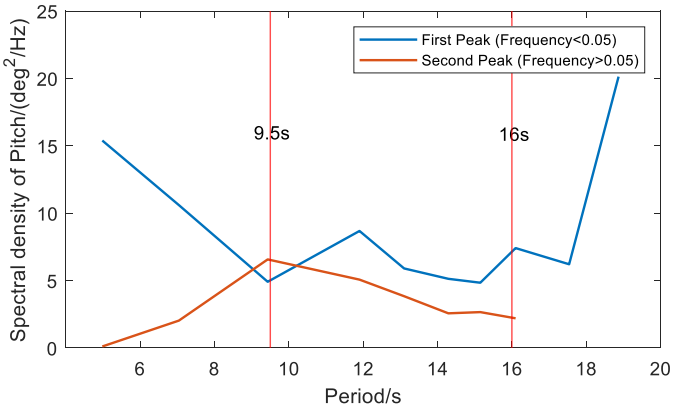

(b) $H_s = 7.1\ m$

FIGURE 8: EXTREME SPECTRAL DENSITY VARIATION OF FIRST AND SECOND PEAKS UNDER A RANGE OF WAVE PERIODS.

It is apparent that the pitch motion of spectral density under the two wave heights has almost the same trend. The first peak could dominate during the wave period a range between 4.98 s to 18.87 s. The second peak shows a trend of increasing and then decreasing with the increase of the wave period, which reaches the maximum value at the wave period of 9.43 s. As the significant wave height increases to 7.1 m, the first and second peaks become much higher.

There are three areas identified in the two figures. In the first area (wave period less than 9.5 s), the first peak shows a downward trend while the second peak increases. In the second area (wave period between 9.5s and 16s), the changes of the first and second peaks are not significant according to the change in the wave period, similar to the results of Fig. 4 (b). In addition, the first and second peak are close in this area. A difference between the two figures in this area is that the second peak could be larger than the first peak when the significant wave height is 7.1 m. In the third area (wave period more than 16s), the first peak increase dramatically with the increasing wave period. There is only the first peak in this area, similar to Fig. 7 (a).

3.3 AERO-HYDRODYNAMIC ANALYSIS

Based on the hydrodynamic time-domain results, the increasing wave height could increase the amplitude of the pitch motion, whilst the varying wave period has a slight influence when it is less than 20 s. Thus, three different wave heights and four different wave periods are chosen for the analysis. As suggested by IEC standard [32], the wind speed intervals should be equal to or less than 2 m/s. Table 5 shows the details of design load cases (27 simulations). Four wave conditions correspond to each wind speed, including wave heights of 0 (wind-only states), 4.73 m, 6 m, and 7.1 m. The cut-in, rated, and cut-out wind speeds of the turbine are 8 m/s, 10.59 m/s, and 25 m/s, respectively.

TABLE 5: THE DESIGN LOAD CASES FOR AERODYNAMIC STUDY

Wind speed (m/s)	Significant wave height (m)			Peak Periods (s)
8	4.73	6	7.1	7.04
10.59	4.73	6	7.1	9.43
12	4.73	6	7.1	11.9
14	4.73	6	7.1	11.9
16	4.73	6	7.1	14.29
18	4.73	6	7.1	14.29
20	4.73	6	7.1	11.9
22	4.73	6	7.1	11.9
25	4.73	6	7.1	14.29

Fig. 9 shows the mean offsets of the platform pitch. The mean offsets under different wave heights are identical but change with the varying wind speeds. The offset increases with the increase of wind speed and reaches its maximum at the wind speed of 14 m/s, whilst the contrary trend can be observed when the wind speed keeps growing. The variation and peak of the displacement is probably caused by the turbine thrust force. The

change in the mean offset is not remarkable when the wind speed is above 14 m/s.

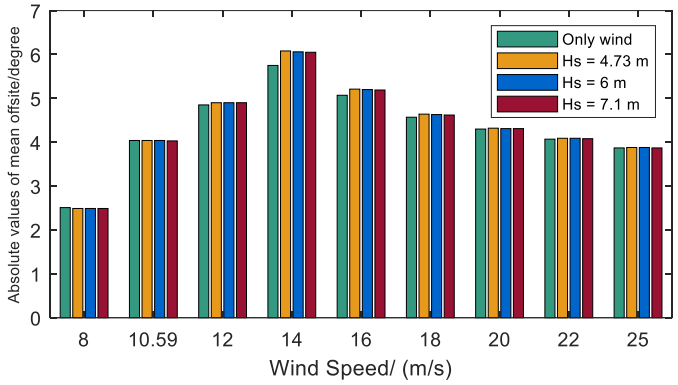

FIGURE 9: ABSOLUTE VAULE OF MEAN PITCHING OFFSET.

Fig. 10 shows the boxplot of the pitch motion amplitude from the equilibrium position. It is observed that the wind and wave influence the dynamic amplitude jointly—the larger wave height results in the more significant pitch motion. Similar to the trend of Fig. 9, the maximum amplitude value occurs at the wind speed of 14 m/s and then decreases with the increasing wind speed. When the wind speed is more than 14 m/s, the dynamic amplitude of the pitch motion remains unchanged, and the conditions with wave effects leads to a more significant pitch motion. For the wind-only condition, it generally has relatively small pitch amplitude.

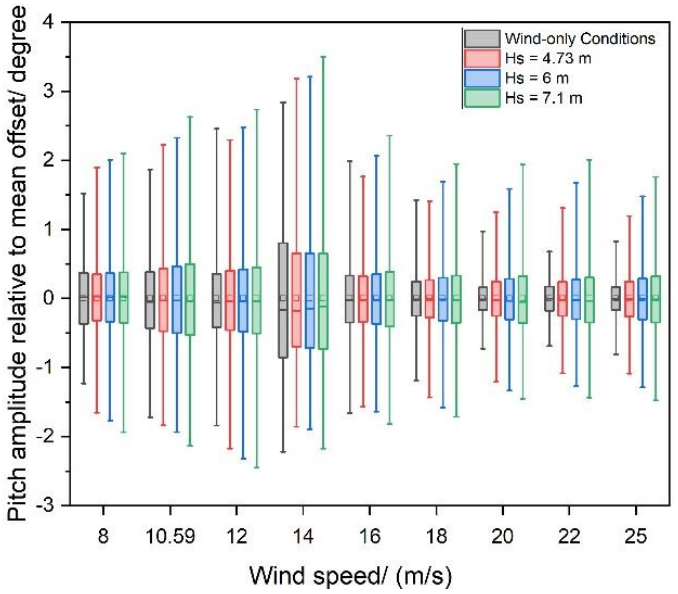

FIGURE 10: PITCH MOTION AMPLITUDE RELATIVE TO THE MEAN OFFSET POSITION.

The standard deviation is presented in Fig 11, in order to further study the effects of aerodynamics on the pitch motion. The larger standard deviation demonstrates a more unstable motion characteristic. The standard deviation of the pitch (Fig. 11) shows an increase and then a decreasing trend for the four conditions. The wind speed of 14 m/s causes the maximum standard deviation, and the standard deviation of wind-only conditions is larger than that of other conditions leading to a more significant pitch motion. Except for that, the standard deviation is smaller than other conditions. Notably, when the wind speed is 8 m/s, 18 m/s, 22 m/s, and 25 m/s, the standard deviation is almost identical except for the wind-only conditions. Particularly, the standard deviation value does not change with the wind speed above 20 m/s.

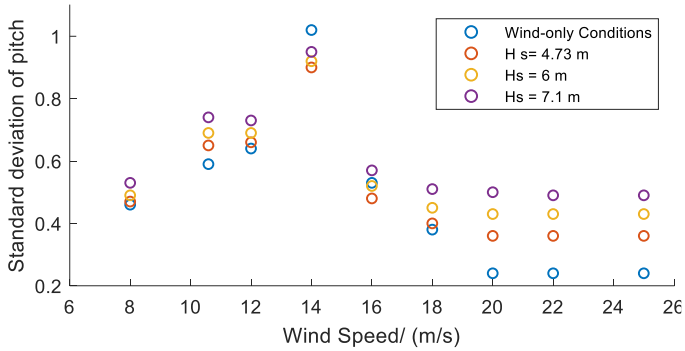

FIGURE 11: STANDARD DEVIATION OF PITCH.

4. DISCUSSION

This paper performed dynamic analysis of the FOWT to discuss the necessity of introducing the damper system.

Based on the hydrodynamic results, the motion response of the FOWT is analyzed. The previous studies show that the damper system is commonly installed in the nacelle of the wind turbine or the platform. The slight motion difference might be between the platform and the wind turbine. This is because the tower is modelled using a line element with high stiffness in Orcaflex. In this study, the damper system will be considered to be installed in the nacelle and the platform, respectively, to enhance the stability of the structure.

The results shown in Fig. 3 and Fig. 4 identify the pitch motion to be damped by potentially employing a damper system. The motion of roll, yaw, and sway can be ignored because the excitation at these motions might be considerably not significant with the wave heading towards the wind turbine. However, when the incident wave direction changes, other motions, such as roll, might become critical [33]. FOWT should have the stability under various conditions. The maximum angle of inclination in roll and pitch is limited to 10 degrees [34], [35].Therefore, a dual or multiple-damper system, consisting of more than one damper, each acting in a single-direction, may be required [13], [33].

From the results of Fig. 3 and Fig. 4, the significant wave height plays a crucial role in the motion amplitude of pitch as the pitch motion amplitude increases remarkably when the significant wave height becomes higher. Besides, the wave period could excite the significant amplitude of pitch motion. This is because the wave period is close to the natural period of pitch motion.

Based on the frequency-domain results of hydrodynamic study, two dominant peaks in the spectral density plots are identified at low and high frequency regions, respectively. According to Fig. 5-Fig. 7, the first peaks are induced by the loads at the natural frequency, leading to structural resonance. Even small second-order hydrodynamic loads may cause a significant resonant effect, which plays a crucial role in the global response of the semi-submersible [36]. The second peaks occur around the wave frequency induced by the first-order wave loads. The two components contribute to the pitch motion in Fig. 4(b).

Fig. 8 exhibits that the first peak is higher than the second peak, especially in the first and third areas. Notably, only the first peak, induced by the first-order wave loads, is in the third area. This may be because the wave frequency is close to the natural frequency of pitch motion, and the frequency of difference frequency loads is not within the range which can excite the structural motion.

Similarly, according to Fig. 7(a), the focus should be given to the natural frequency of the pitch motion when the wave period is larger than 18.87s. For this particular case, the single damper system may be effective and economical in motion reduction. Notably, the normal wave period range is from 5 s to 20 s. As for the single damper system, the natural frequency of the device is tuned to the natural frequency of the structural motion to maximize energy absorption, which is the most important aspect of designing the damper system [16]. Meanwhile, the results also indicate that the second peak could be close to or larger than the first peak. Overall, both the first and second peaks have a significant effect on the stabilization of the wind turbine. Based on these observations, the dual damper system is proposed as an effective and generally applicable strategy to reduce both the resonance at the natural frequency and oscillations at the wave frequency.

Wind loads could be crucial for the dynamic performance of the FOWT. Generally, the tower of the FOWT can exceed 100 m in height. Even small pitch motions can cause a critical dynamic effect, leading to worse tower excursions [6]. The results of Fig. 9 illustrate that only wind could change the mean offsets of the FOWT. For a damper system, it does not affect the mean offsets of the structure. Therefore, the mean offsets are taken off in the following results of Section 3.3.

The global displacement and load related to the inflow wind, are mainly dependent on the turbine thrust force which could lead to large pitch amplitude and standard deviation simultaneously. However, the values could be relatively small. This is because the blade pitch control strategy increases the blade pitch angle when the wind speed is close to the cut-out speed. The aerodynamics has less effect on the pitch motion when the wind speed is more than 14 m/s, demonstrating that the effect of wave height is dominant at this stage. Compared with Fig. 3 (wave heights of 4.73 m, 6 m, and 7.1 m), the increase in pitch amplitude is not prominent after introducing wind loads. For instance, the amplitude in Fig.3 at the wave height of 7.1 m is approximately 2.2 degrees, and the same value can be observed in Fig. 10. According to the above results, the wind loads can result in a large offset but fewer effects on the pitch amplitude when the wind speed is more than 14 m/s. Therefore, it could be possible to give much attention on the wave effects when designing or verifying a damper system, as the damper system could only affect the amplitude. For example, the wind speed could be set to be fixed at 14 m/s in order to assess the capability of the damper system.

Overall, the aerodynamic and hydrodynamic significantly affect the motion stabilization of the FOWT with varying environmental conditions. These observations show that wave effects could dominate the pitch motion responses. Additionally, tower bending moments, another critical design component, will be investigated and introduced to identify the effectiveness of the damper system in the following studies. A dual damper system is proposed as an effective and generally applicable strategy to reduce both resonances at the natural frequency and oscillations at the wave frequency.

5. CONCLUSION

In this paper, the dynamic analysis of the IEA 15 MW semi-submersible FOWT has been conducted under a range of environmental conditions to demonstrate the wind and wave effects, and the requirements of introducing a damper system. Two dominant peaks of spectral density are observed. Wind loads could be less effect on the motion amplitude under certain conditions. A dual damper system or multiple damper system is suggested to be employed for better motion stabilization of the structure. The results of the dynamic analysis can be the basis for applying the damper system.

Future work will concentrate on the damper system. According to the current results, a mathematical model will be established and simplified with reduced DOFs and limited external loads. The passive damper will be investigated first and introduced to the mathematical model. The damper properties, including the mass, natural frequency, stiffness, and damping, are optimized based on the targeted functions related to the motion responses of the FOWT. The verification of the damper approach will be conducted based on both normal and extreme conditions. The study will also include the method of introducing the damper system to Orcaflex. The results of this study will be used to evaluate the efficiency of the damper system. For better applicability and effectiveness of the damper system, the multiple-directions damper system and active damper will be investigated subsequently.

REFERENCES

[1] P. Zhang *et al.*, ‘Dynamic Response of Articulated Offshore Wind Turbines under Different Water Depths’, *Energies*, vol. 13, no. 11, p. 2784, Jun. 2020, doi: 10.3390/en13112784.

[2] A. Jamalkia, M. M. Ettefagh, and A. Mojtahedi, ‘Damage detection of TLP and Spar floating wind turbine using dynamic response of the structure’, *Ocean Eng.*, vol. 125, pp. 191–202, Oct. 2016, doi: 10.1016/j.oceaneng.2016.08.009.

[3] E. Uzunoglu and C. Guedes Soares, 'On the model uncertainty of wave induced platform motions and mooring loads of a semisubmersible based wind turbine', *Ocean Eng.*, vol. 148, pp. 277–285, Jan. 2018, doi: 10.1016/j.oceaneng.2017.11.001.

[4] A. Myhr, C. Bjerkseter, A. Ågotnes, and T. A. Nygaard, 'Levelised cost of energy for offshore floating wind turbines in a life cycle perspective', *Renew. Energy*, vol. 66, pp. 714–728, Jun. 2014, doi: 10.1016/j.renene.2014.01.017.

[5] T. Stehly and P. Duffy, '2020 Cost of Wind Energy Review', *Renew. Energy*, 2022.

[6] A. Nazokkar and R. Dezvareh, 'Vibration control of floating offshore wind turbine using semi-active liquid column gas damper', *Ocean Eng.*, vol. 265, p. 112574, Dec. 2022, doi: 10.1016/j.oceaneng.2022.112574.

[7] L. Zhang, W. Shi, M. Karimirad, C. Michailides, and Z. Jiang, 'Second-order hydrodynamic effects on the response of three semisubmersible floating offshore wind turbines', *Ocean Eng.*, vol. 207, p. 107371, Jul. 2020, doi: 10.1016/j.oceaneng.2020.107371.

[8] S. Sarkar and B. Fitzgerald, 'Vibration control of spar-type floating offshore wind turbine towers using a tuned mass-damper-inerter', *Struct. Control Health Monit.*, vol. 27, no. 1, Jan. 2020, doi: 10.1002/stc.2471.

[9] Z. Zhao, X. Li, W. Wang, and W. Shi, 'Analysis of Dynamic Characteristics of an Ultra-Large Semi-Submersible Floating Wind Turbine', *J. Mar. Sci. Eng.*, vol. 7, no. 6, Art. no. 6, Jun. 2019, doi: 10.3390/jmse7060169.

[10] S. Park, M. A. Lackner, P. Pourazarm, A. Rodríguez Tsouroukdissian, and J. Cross-Whiter, 'An investigation on the impacts of passive and semiactive structural control on a fixed bottom and a floating offshore wind turbine', *Wind Energy*, vol. 22, no. 11, pp. 1451–1471, 2019, doi: 10.1002/we.2381.

[11] S. Colwell and B. Basu, 'Tuned liquid column dampers in offshore wind turbines for structural control', *Eng. Struct.*, vol. 31, no. 2, pp. 358–368, Feb. 2009, doi: 10.1016/j.engstruct.2008.09.001.

[12] M. A. Lackner and M. A. Rotea, 'Passive structural control of offshore wind turbines', *Wind Energy*, vol. 14, no. 3, pp. 373–388, Apr. 2011, doi: 10.1002/we.426.

[13] G. Stewart and M. Lackner, 'Offshore Wind Turbine Load Reduction Employing Optimal Passive Tuned Mass Damping Systems', *IEEE Trans. Control Syst. Technol.*, vol. 21, no. 4, pp. 1090–1104, Jul. 2013, doi: 10.1109/TCST.2013.2260825.

[14] C. Li, T. Zhuang, S. Zhou, Y. Xiao, and G. Hu, 'Passive Vibration Control of a Semi-Submersible Floating Offshore Wind Turbine', *Appl. Sci.*, vol. 7, no. 6, Art. no. 6, Jun. 2017, doi: 10.3390/app7060509.

[15] A. Hemmati, E. Oterkus, and M. Khorasanchi, 'Vibration suppression of offshore wind turbine foundations using tuned liquid column dampers and tuned mass dampers', *Ocean Eng.*, vol. 172, pp. 286–295, Jan. 2019, doi: 10.1016/j.oceaneng.2018.11.055.

[16] D. Villoslada, M. Santos, and M. Tomás-Rodríguez, 'TMD stroke limiting influence on barge-type floating wind turbines', *Ocean Eng.*, vol. 248, p. 110781, Mar. 2022, doi: 10.1016/j.oceaneng.2022.110781.

[17] M. L. Brodersen, A.-S. Bjørke, and J. Høgsberg, 'Active tuned mass damper for damping of offshore wind turbine vibrations: Active tuned mass damper for damping of offshore wind turbine vibrations', *Wind Energy*, vol. 20, no. 5, pp. 783–796, May 2017, doi: 10.1002/we.2063.

[18] Y. Hu and E. He, 'Active structural control of a floating wind turbine with a stroke-limited hybrid mass damper', *J. Sound Vib.*, vol. 410, pp. 447–472, Dec. 2017, doi: 10.1016/j.jsv.2017.08.050.

[19] B. Fitzgerald, S. Sarkar, and A. Staino, 'Improved reliability of wind turbine towers with active tuned mass dampers (ATMDs)', *J. Sound Vib.*, vol. 419, pp. 103–122, Apr. 2018, doi: 10.1016/j.jsv.2017.12.026.

[20] 'OrcaFlex Help'. https://www.orcina.com/webhelp/OrcaFlex/ (accessed May 14, 2023).

[21] E. Gaertner *et al.*, 'Definition of the IEA 15-Megawatt Offshore Reference Wind Turbine', National Renewable Energy Laboratory (NREL), Report, 2020.

[22] Z. Cheng, H. A. Madsen, Z. Gao, and T. Moan, 'A fully coupled method for numerical modeling and dynamic analysis of floating vertical axis wind turbines', *Renew. Energy*, vol. 107, pp. 604–619, Jul. 2017, doi: 10.1016/j.renene.2017.02.028.

[23] S. Gueydon, T. Duarte, and J. Jonkman, 'Comparison of Second-Order Loads on a Semisubmersible Floating Wind Turbine', in *Volume 9A: Ocean Renewable Energy*, San Francisco, California, USA: American Society of Mechanical Engineers, Jun. 2014, p. V09AT09A024. doi: 10.1115/OMAE2014-23398.

[24] C. Allen *et al.*, 'Definition of the UMaine VolturnUS-S Reference Platform Developed for the IEA Wind 15-Megawatt Offshore Reference Wind Turbine', NREL/TP--5000-76773, 1660012, MainId:9434, Jul. 2020. doi: 10.2172/1660012.

[25] B. J. Jonkman, 'TurbSim User's Guide v2.00.00', *Renew. Energy*, 2014.

[26] Z.-F. Fu and J. He, *Modal Analysis*. Elsevier, 2001.

[27] 'Modal analysis: Theory'. https://www.orcina.com/webhelp/OrcaFlex/Content/html/Modalanalysis,Theory.htm (accessed May 19, 2023).

[28] Z. Liu, Q. Zhou, Y. Tu, W. Wang, and X. Hua, 'Proposal of a Novel Semi-Submersible Floating Wind Turbine Platform Composed of Inclined Columns and Multi-Segmented Mooring Lines', *Energies*, vol. 12, no. 9, p. 1809, May 2019, doi: 10.3390/en12091809.

[29] B. Liu and J. Yu, 'Effect of Mooring Parameters on Dynamic Responses of a Semi-Submersible Floating Offshore Wind Turbine', *Sustainability*, vol. 14, no. 21, p. 14012, Oct. 2022, doi: 10.3390/su142114012.

[30] F. Lemmer, ‘7.5 Guidance on platform and mooring line selection, installation and marine operations’.
[31] L. Zhang, W. Shi, Y. Zeng, C. Michailides, S. Zheng, and Y. Li, ‘Experimental investigation on the hydrodynamic effects of heave plates used in floating offshore wind turbines’, *Ocean Eng.*, vol. 267, p. 113103, Jan. 2023, doi: 10.1016/j.oceaneng.2022.113103.
[32] ‘IEC TS 61400-3-2:2019 | IEC Webstore’. https://webstore.iec.ch/publication/29244 (accessed May 03, 2023).
[33] V.-N. Dinh and B. Basu, ‘Passive control of floating offshore wind turbine nacelle and spar vibrations by multiple tuned mass dampers: PASSIVE CONTROL OF FLOATING WIND TURBINES BY MTMDs’, *Struct. Control Health Monit.*, vol. 22, no. 1, pp. 152–176, Jan. 2015, doi: 10.1002/stc.1666.
[34] M. Collu and M. Borg, ‘11 - Design of floating offshore wind turbines’, in *Offshore Wind Farms*, C. Ng and L. Ran, Eds., Woodhead Publishing, 2016, pp. 359–385. doi: 10.1016/B978-0-08-100779-2.00011-8.
[35] E. N. (Elizabeth N.) Wayman, ‘Coupled dynamics and economic analysis of floating wind turbine systems’, Thesis, Massachusetts Institute of Technology, 2006. Accessed: Sep. 05, 2023. [Online]. Available: https://dspace.mit.edu/handle/1721.1/35650
[36] A. J. Couling, A. J. Goupee, A. N. Robertson, and J. M. Jonkman, ‘Importance of Second-Order Difference-Frequency Wave-Diffraction Forces in the Validation of a Fast Semi-Submersible Floating Wind Turbine Model: Preprint’, National Renewable Energy Lab. (NREL), Golden, CO (United States), NREL/CP-5000-57697, Jun. 2013. doi: 10.1115/OMAE2013-10308.